JOURNAL OF MATERIALS SCIENCE **37** (2002) 2421 – 2426

Wet erosion behaviour of low SiC alumina-SiC nanocomposites

H. KARA*, S. G. ROBERTS
Department of Materials, University of Oxford, Oxford, OX1 3PH, UK
E-mail: steve.roberts@materials.ox.ac.uk

We have investigated the erosive wear behaviour of alumina and Al_2O_3-SiC "nanocomposites" with SiC content between 1 and 5%. Nanocomposites (grain sizes between 3.15 and 7.16 μm) and alumina (grain size 4.43 μm) were eroded with SiC particles using a custom-built erosive slurry wear tester. The erosion resistance of the nanocomposites increased slightly with decreasing grain size. Nanocomposites of all grain sizes showed better wear resistance than the alumina. Erosion resistance increases with SiC content, though this effect is not strong for SiC contents greater than 2%. These results are compared with related results from the literature.

1. Introduction

Technical ceramics are of great importance in industrial applications where the degradation of components by particles is a problem, i.e. large-scale handling of aggregates and slurries in industrial operations. Solid particle erosion of ceramics and material removal processes from surfaces have been studied by several researchers [1–9]. Much of this work has been carried out on alumina, as it is the most used technical ceramic in industry. Erosion tests may be performed using high-speed airborne particles (e.g. by Shipway and Hutchings [3]) or using lower-speed liquid-borne particles (e.g. Franco and Roberts [7]). The erosion rate of polycrystalline alumina is grain-size dependent [7–9], with higher erosion rates at larger grain sizes. Grain detachment is more probable for larger grain sizes and grit sizes [8, 9]. The apparatus used by Franco and Roberts [7, 9] allowed control of the impact angle of the erodent particles. They found that erosion rate varied with the particle velocity normal to the surface, V_n, proportionally to $V_n^{2.4}$.

Generally, material is lost from ceramic surfaces via lateral fracture from impact sites. At high impact speeds (e.g. in airborne particle erosion), individual erodent particles strike with enough energy to cause immediate material loss; such processes have been modelled by, e.g., Evans and Wilshaw [10]. At the lower speeds used in slurry erosion testing [7–9], there is some evidence that multiple adjacent impacts are needed to remove material [11].

Fine SiC particles (up to 20%) can be incorporated into alumina to produce a "nanocomposite" [12]. The resulting material can have substantially improved strength [12–14] and possibly toughness [12, 13], and better surface quality after polishing [15, 18]. It appears that the nanocomposites gain strong surface residual stresses in grinding and lapping [19], because of differences in subsurface deformation mechanism [20]. These may account for the strength improvements. Davidge *et al.* [13] conducted wet erosive wear tests on alumina and alumina/SiC nanocomposites with 5–20% SiC volume content and concluded that the addition of SiC into alumina has beneficial effects on wear resistance. Similar results were reported by Sternitzke *et al.* [16], who reported an influence of incorporated SiC particle size, with the finest SiC particles giving the best wear resistance.

The addition of as little as 1% SiC into alumina improves the surface quality after lapping and polishing to a great extent compared with pure alumina [15]. Al_2O_3-SiC nanocomposite materials with low SiC content might therefore have high free-particle erosive and abrasive wear resistance. In this study we investigate the wet erosive wear properties of alumina-SiC nanocomposites with 1–5% SiC compared with those of pure alumina. The effect of grain size on erosive wear rate was also examined.

2. Experimental procedure

2.1. Material preparation and characterisation

The production method used to prepare alumina and its nanocomposites is given in detail elsewhere [13]. Here a short description is given. 1–5% vol. of α-SiC reinforcement with an average particle size of 200 nm (UF 45 - Lonza, Germany) was dispersed ultrasonically for 20 minutes and mixed with α-Al_2O_3 of 400 nm average particle size (AES11C - Sumitomo, Japan). The mixture was then attrition milled in distilled water for 2 hours. The resulting slurry was vacuum dried for 24 hours followed by 4 hours freeze-drying. Powders were then sieved through a 150 μm mesh. The same treatment was also applied to alumina powders.

* *Present Address:* Department of Engineering & Applied Science, University of Bath, Bath BA2 7AY, UK.

TABLE I Properties of alumina and Al_2O_3/SiC nanocomposites

SiC content (volume%)	Density (g/cm^3)	Density[a](%)	Porosity[b](%)	Grain size (μm)	E (GPa)	Poisson's ratio (ν)
0	3.920 ± 0.02	99.94 ± 0.11	0.58 ± 0.13	4.43 ± 0.22	373 ± 5.5	0.25
1	3.928 ± 0.06	99.62 ± 0.66	0.19 ± 0.11	7.16 ± 0.16	408 ± 3.5	0.25
2	3.918 ± 0.04	99.45 ± 0.72	0.50 ± 0.14	5.90 ± 0.53	387 ± 2.1	0.25
3	3.932 ± 0.02	100 ± 0.00	0.53 ± 0.04	4.34 ± 0.14	385 ± 1.0	0.25
4	3.909 ± 0.01	99.73 ± 0.20	0.89 ± 0.06	3.72 ± 0.10	379 ± 1.6	0.25
5	3.866 ± 0.01	99.50 ± 0.82	1.40 ± 0.18	3.15 ± 0.16	363 ± 8.3	0.25

[a]From Archimedes' method.
[b]Calculated from SEM micrographs.

Alumina and Al_2O_3/SiC nanocomposite powders were uniaxially pressed at 40 MPa compaction pressure using a 36 mm diameter stainless steel die. Sintering was performed in a 37 mm diameter alumina tube furnace in a flowing nitrogen atmosphere for 2 hours at 1600°C for alumina and 1700°C for nanocomposites. All nanocomposite compacts were embedded in a 750 μm SiC bed, whereas alumina compacts were placed in an alumina bed. The heating and cooling rate was 3°C/min., to avoid thermal-shock cracking in the sintered ceramic body.

The materials' properties are given in Table I. The densities of the compacts were determined by Archimedes' method using distilled water as an immersion medium at room temperature. All samples were boiled for saturation for 1 hour prior to measurement. The relative density values were calculated using the theoretical densities of α-Al_2O_3 (3.96 gcm^{-3}) and α-SiC (3.05 gcm^{-3}). Grain size measurements were made by a linear intercept method counting at least 600 intercepts on SEM micrographs. Elastic properties (Young's modulus, E and Poisson's ratio, ν) were measured by a resonance method using a "Grindosonic" MK5 Industrial machine (J. W. Lemmens, Belgium).

Fig. 1 shows the microstructures of alumina and alumina-5% SiC nanocomposite. There is a refinement in grain size with the addition of SiC particles but these particles are also responsible for retarding densification. This is apparent in Fig. 1b and Table I where the addition of 5% SiC leaves a number of pores (1.4%) within the microstructure. Pores were traced from the SEM micrographs and pore fraction calculated using an image analyser (Kontronik, Germany). The area fraction of pores is plotted against SiC content in Fig. 2. There is a near-linear relation between pore density and SiC content. The alumina (sintered at a lower temperature) has 0.55% pore volume. Besides retarding densification, SiC particles can cause agglomeration if the powder processing is not handled carefully. This was observed, in particular, in 2% SiC material during SEM investigations. This was probably due to be a leakage during vacuum drying allowing SiC particles to settle on the bottom of the flask.

2.2. Wet erosion testing

The erosion testing machine used (see Fig. 3) was constructed and calibrated in the Department of Materials, University of Oxford [7, 9]. It consists of sample holder revolving in a large slurry pot. The sample holder is mounted on one end of a 275 mm stainless steel arm attached to a stainless steel shaft connected to a motor. At the other end of the arm a stainless steel paddle is attached to mix the slurry. Both the sample holder and the paddle rotate in a groove delimited by the pot's inner wall and a fibre-glass cylinder in the centre of the pot. The groove width is 65 mm and the sample holder rotates 20 mm from the bottom of the pot within the groove, at speeds ranging from 10 to 200 rpm. A buffer system (8 radial blades) is mounted 3 mm above the rotating arm in order to prevent the slurry from rotating with the sample holder.

The slurry used consisted of 8 litres of water and 1500 g of SiC with 780 μm mean particle size. The sample holder (made of nylon) has a funnel-shaped slurry collection zone which channels erodent particles onto a well-defined circular region ($\sim$5 mm diameter) of the specimen surface. The SiC particles strike the material surface at normal incidence. Particle velocity was calibrated in an earlier set of experiments [7] to be 2.4 ± 1.5 ms^{-1} at 120 rpm, the rotation speed used in these experiments (the error reflects uncertainty in various parameters used in the calibration method: the velocity is very consistent from one experiment to the next at the same rotational speed) . Material losses from the surface were measured by weighing before testing, after one hour and then at 2 hour intervals up to 13 hours in total. The measured wear scar sizes were used to calculate an average loss rate in nms^{-1}. Wear scars were examined by SEM to study material loss mechanisms.

3. Erosion results and discussion

Eroded surfaces of alumina and alumina/SiC nanocomposites with various SiC additions are shown in Fig. 4. The eroded surfaces of alumina-SiC nanocomposites are different from those of alumina. In alumina, sharp grain edges and deep holes (Fig. 4a) are clear indications that the material lost from the surface is mainly due to grain detachment and intergranular fracture. For the nanocomposites (Fig. 4b–d), though there is some material loss by grain detachment, the images show predominantly smooth surfaces resulting from transgranular fracture. All nanocomposites exhibited similar eroded surfaces regardless of SiC particle content. The fractions of transgranular (smooth) areas of eroded surfaces were calculated from SEM micrographs and are plotted against SiC volume content in Fig. 5. The change in fracture mode from mainly intergranular in alumina to mainly transgranular in nanocomposite is apparent; SiC additions as low as 1% can promote this behaviour. Above 1%, SiC content does not seem to have a pronounced effect on the amount of transgranular fracture.

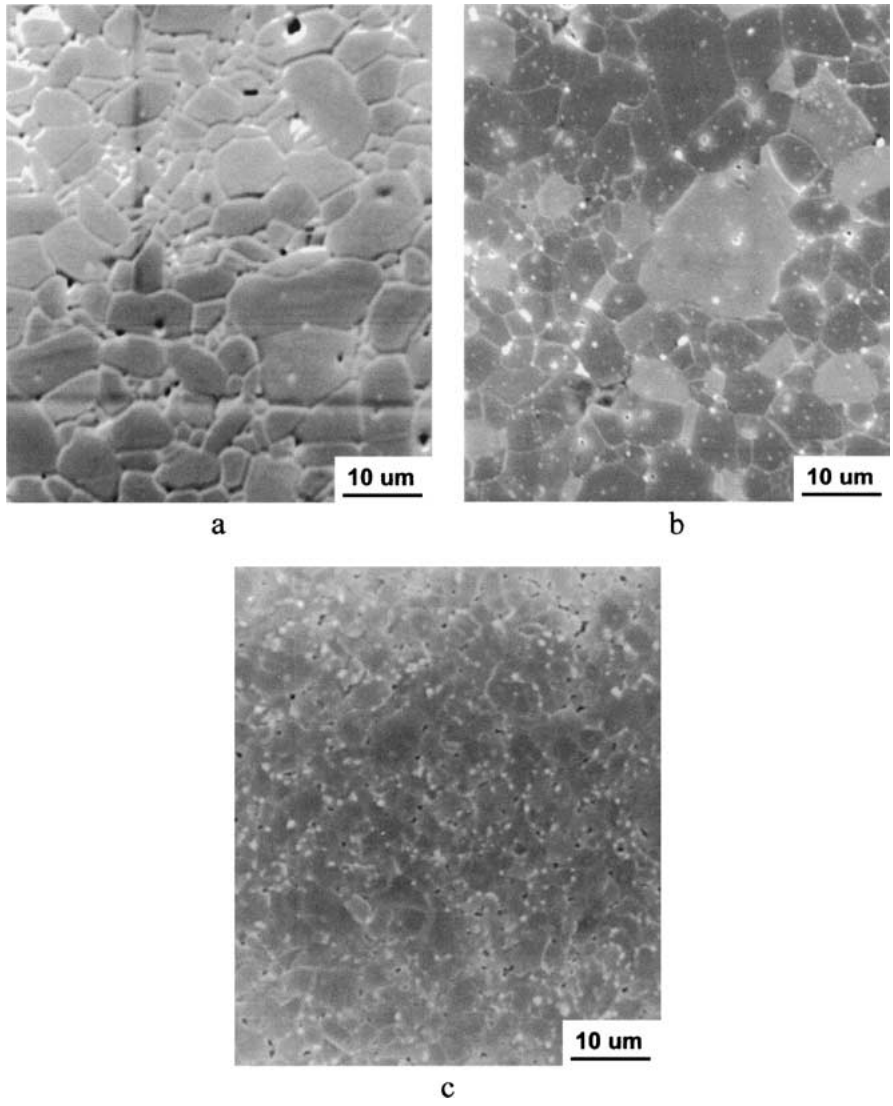

Figure 1 Microstructures of (a) alumina (b) alumina/1% SiC nanocomposite, and (c) alumina/5% SiC nanocomposite (SEM secondary images of thermally-etched surfaces).

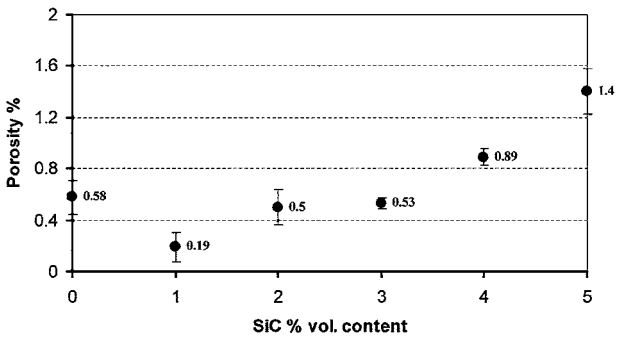

Figure 2 Variation in pore volume with SiC particle content after sintering of alumina (1600°C) and alumina/SiC nanocomposites (1700°C).

Erosion rate results are given in Table II, together with the results obtained by Franco and Roberts [9] on alumina and Davidge *et al.* [18] on nanocomposites. Results are plotted against SiC volume content in Fig. 6. The nanocomposite materials are generally more resistant to erosion wear than pure alumina, though there are considerable differences in data from different studies. This may be due to differences in the test method used (in the work of Davidge *et al.* [18], the incident angle

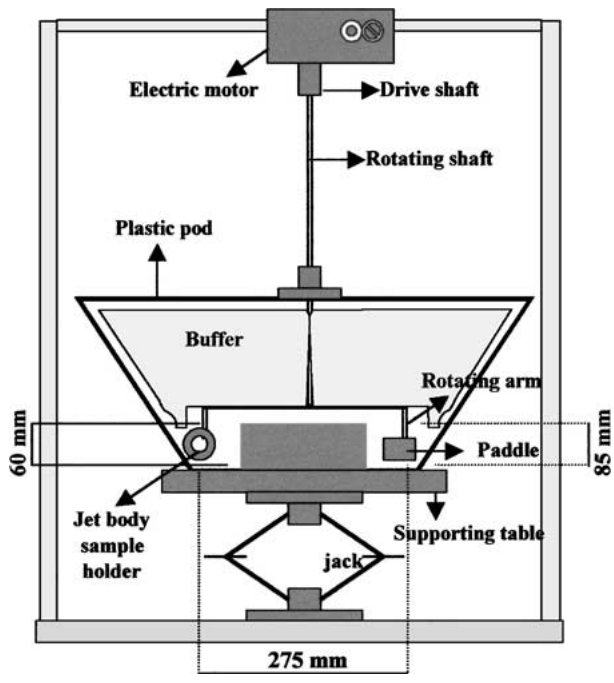

Figure 3 Schematic diagram of erosive wear tester used in the study (after [9]).

TABLE II Wet erosion test results for alumina and alumina/SiC nanocomposites

Material	Grain size (μm)	Erosion rate nm s^{-1}	Notes
Al_2O_3	1.2 ± 0.50	1.83 ± 0.7	Data from Franco and Roberts [9]. α-alumina (AKP-50, Sumitomo), normal incidence, particle speed = 2.4 ms^{-1}. 11 hours of exposure time.
Al_2O_3	3.8 ± 0.80	8.36 ± 0.8	
Al_2O_3	14.1 ± 1.5	11.3 ± 0.6	
Al_2O_3	4.43 ± 0.22	4.51	Data from this study. AES 11C α-alumina, normal incidence with a particle speed of 2.4 ms^{-1}. 13 hours of exposure time.
Al_2O_3-1% SiC	7.16 ± 0.14	3.29	
Al_2O_3-2% SiC	5.90 ± 0.53	6.03	
Al_2O_3-3% SiC	4.34 ± 0.14	2.19	
Al_2O_3-4% SiC	3.72 ± 0.10	1.84	
Al_2O_3-5% SiC	3.15 ± 0.16	2.23	
Al_2O_3-5% SiC	0.5	1.2	Data from Davidge *et al.* [13]. α-alumina (AKP-53, Sumitomo). Wide range of impact angles and impact speeds. Fused alumina erodent. 6 hours of exposure time.
Al_2O_3-10% SiC	0.8	1.4	
Al_2O_3-20% SiC	0.4	5.9	

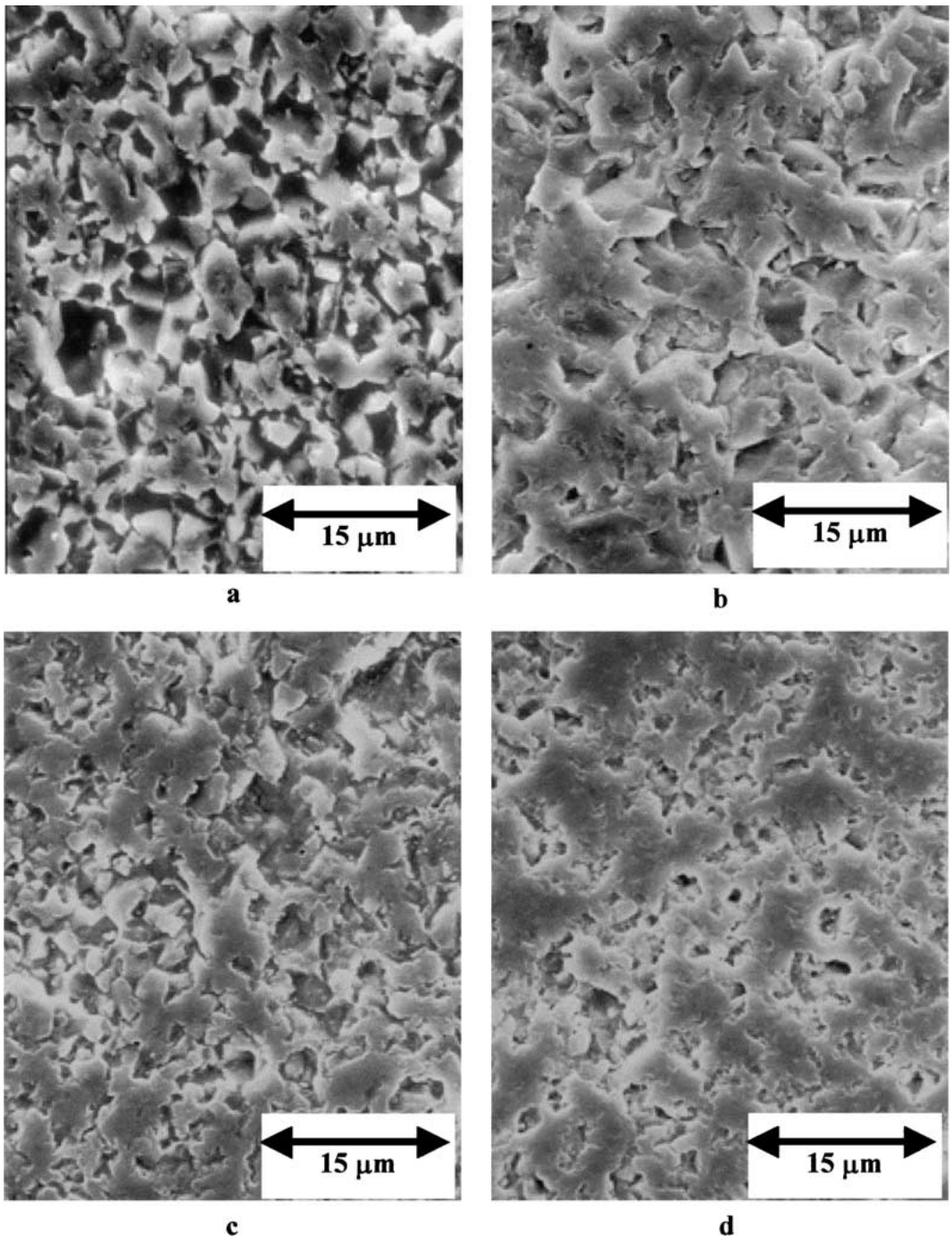

Figure 4 SEM micrographs of eroded surfaces of (a) alumina, (b) 1% SiC, (c) 3% SiC, and (d) 5% SiC nanocomposites after 13 hours of testing.

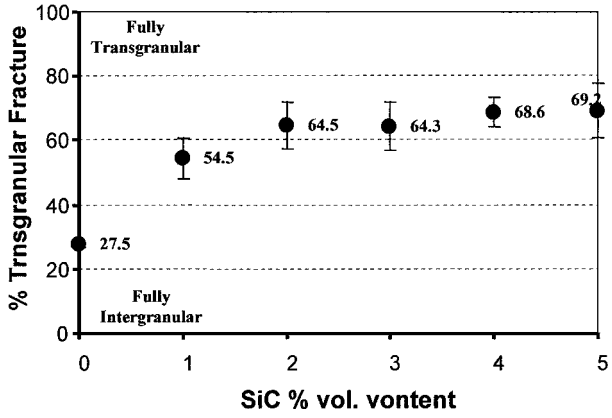

Figure 5 Variation of transgranular fracture surface area with SiC volume content after wet erosion tests of 13 hours.

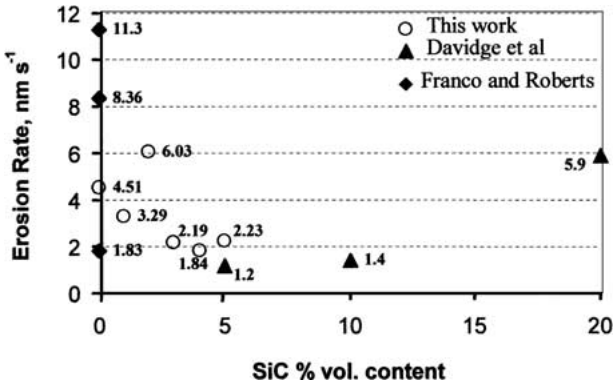

Figure 6 Variation in slurry erosion rate with SiC volume content for alumina and nanocomposites, comparised with other researchers' results. Numbers shown by each data point indicate mean grain size (μm).

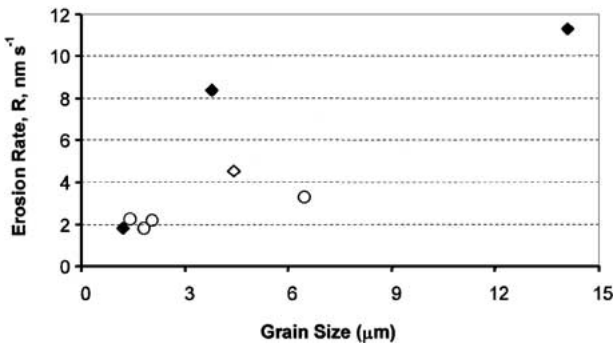

Figure 7 Wear erosion rate data using the Oxford testing equipment, for fully dense nanocomposite materials and pure alumina (2% SiC data not shown; SiC agglomeration gives anomalous results). ♦ alumina (Franco and Roberts), ◇ alumina (this study) and ○ nanocomposite

was uncontrolled) or to difference in materials and production routes used. Nanocomposites with SiC content in the range 1–10% have similar wear behaviour, with erosion rate falling slightly with increasing SiC content. The exceptions are the 2% and 20% SiC materials, which had, respectively, high SiC agglomeration and a high porosity level (9%).

The alumina materials showed a range of wide wear rates. As all alumina materials are densified to over 99% theoretical density, the variation in wear rates may be at least partly due to variation in grain size [8, 9, 18]. Fig. 7 shows the erosion rates plotted against grain size for alumina and nanocomposites. The alumina materials exhibit strong grain size dependence on erosion, whereas this effect is less pronounced for the nanocomposites. It appears that SiC addition into alumina, in addition to reducing the erosion rate, suppresses the effect of grain size on erosion resistance. For example, alumina with a mean grain size of 4.43 μm had an erosion rate of 4.51 nms^{-1} whereas the 1% SiC nanocomposite, with a bigger average grain size of 7.16 μm, had an erosion rate of 3.29 nms^{-1} (Fig. 6).

There is a considerable amount of scatter in the erosion data, especially for alumina. For hot pressed materials with $\sim$1 μm grain size, the nanocomposites apparently have similar wear resistance to alumina, but the test methods used for the two types of material, tested by different groups are not the same; and a direct comparison is not really possible. However, it is clear that when the same test method is used, in the 3–8 μm grain size range (i.e. for sintered materials) the nanocomposites have approximately 2–3 times the erosion wear resistance of the alumina.

The main effect of the SiC appears to be to increase the strength of the alumina grain boundaries. This suppresses grain removal by grain boundary fracture in erosion, similarly to effects already found in grinding and polishing [15, 19] and in fracture tests [18], and also reduces the dependence on grain size. The mechanisms underlying this grain boundary strengthening remain to be determined, though it appears from the work of Winn and Todd [17] that it is the SiC particles on the boundaries (rather than intragranular SiC) that are responsible for the effect.

4. Summary

1. Incorporation of fine SiC particles into sintered alumina can improve erosive wear resistance, by a factor of 200–300%.

2. This improvement can be gained by the addition of as little as 1% SiC particles; further increases give only slight improvements in wear resistance.

3. Porosity reduces erosive wear resistance and porosity may be produced by sintering with SiC content of 10% or above. Agglomeration of SiC particles also reduces erosion wear resistance.

4. The erosive wear of alumina shows strong grain size dependence but this dependence is less significant in the case of nanocomposites.

5. Material removal from the surface of alumina is mainly by intergranular fracture resulting in grain detachment or dislodgement. However, eroded surfaces of nanocomposites showed $\sim$60% smooth areas indicating intragranular fracture. This is likely to be due to strengthening of grain boundaries by the SiC particles.

Acknowledgment

HK thanks the Turkish Government for financial support.

References

1. J. E. RITTER, in "Erosion of Ceramic Materials," edited by J. E. Ritter (Trans Tech Publications, 1992) p. 93.
2. J. L. ROUTBORT and R. O. SCATTERGOOD, in "Erosion of Ceramic Materials," edited by J. E. Ritter (Trans Tech Publications, 1992) p. 23.

3. P. H. SHIPWAY and I. M. HUTCHINGS, *Wear* **193** (1996) 105.
4. S. LATHABAI, *Materials Forum* **19** (1995) 101.
5. Y. I. OKA, H. OHNOGI, T. HOSOKAWA and M. MATSUMURA, *Wear* **203** (1997) 573.
6. A. F. COLCLOUGH and J. A. YEOMANS, *ibid.* **209** (1997) 229.
7. A. FRANCO and S. G. ROBERTS, *J. Eur. Ceram. Soc.* **18** (1998) 269.
8. M. MIRANDA-MARTINEZ, R. W. DAVIDGE and F. L. RILEY, *Wear* **172** (1994) 41.
9. A. FRANCO and S. G. ROBERTS, *J. Eur. Ceram. Soc.* **16** (1996) 1365.
10. A. G. EVANS and T. R. WILSHAW, *Acta Metall.* **24** (1976) 939.
11. K. NIIHARA, *J. Ceram. Soc. Jpn.* **99** (1991) 974.
12. A. FRANCO, D.Phil. thesis, University of Oxford, 1996.
13. R. W. DAVIDGE, R. J. BROOK, F. CAMBIER, M. POORTEMAN, A. LERICHE, D. O'SULLIVAN, S. HAMPSHIRE and T. KENNEDY, *Brit. Ceram. Transactions* **96**(3) (1997) 121.
14. J. ZHAO, L. C. STEARNS, M. P. HARMER, H. M. CHAN and G. A. MILLER, *J. Amer. Ceram. Soc.* **76**(2) (1993) 503.
15. H. KARA and S. G. ROBERTS, *ibid.* **83** (2000) 1219.
16. M. STERNITZKE, E. DUPAS, P. TWIGG and B. DERBY, *Acta. Mater.* **45**(10) (1997) 3963.
17. A. J. WINN and R. I. TODD, in "Engineering with Ceramics," edited by W. E. Lee and B. Derby, British Ceramic Proceedings No. 59, p. 153.
18. H. Z. WU, C. W. LAWRENCE, S. G. ROBERTS and B. DERBY, *Acta. Mater.* **46**(11) (1998) 3839.
19. H. Z. WU, S. G. ROBERTS and B. DERBY, *Acta Mater.* **49** (2001) 507.
20. H. Z. WU, B. J. INKSON and S. G. ROBERTS, *J. Microsc.* **201** (2001) 212.
21. R. W. DAVIDGE, P. C. TWIGG and F. L. RILEY, *J. Eur. Ceram. Soc.* **16** (1996) 799.

Received 14 August 2001
and accepted 24 January 2002